

Hysteresis in mesoscopic superconducting disks: The Bean-Livingston barrier

P. Singha Deo,* V. A. Schweigert,† and F. M. Peeters‡

Department of Physics, University of Antwerp (UIA), B-2610 Antwerpen, Belgium

(Received 17 November 1998)

Depending on the size of mesoscopic superconducting disks, the magnetization can show hysteretic behavior which we explain by using the Ginzburg-Landau (GL) theory and properly taking into account the demagnetization effects due to geometrical form factors. In large disks the hysteresis is due to the Bean-Livingston surface barrier while in small disks it is the volume barrier which is responsible for it. Although the sample magnetization is diamagnetic (negative) we show that the measured magnetization can be positive at certain fields as observed experimentally and which is a consequence of both the demagnetization effect and the experimental setup. [S0163-1829(99)04009-6]

Hysteresis in the magnetization of superconductors¹⁻³ is a fascinating field of fundamental research which is related to the occurrence of metastability. Here we will investigate this phenomenon in *single* mesoscopic superconducting disks. Recently, Geim *et al.*⁴ used the Hall probe technique to study the magnetization of single mesoscopic Al disks. The investigated disks can be classified as few fluxoid disks (FwFD) and fractional fluxoid disks (FrFD). The FrFD are so tiny that fluxoids cannot nucleate because the required magnetic field to create a fluxoid exceeds the critical field of the sample. The FwFD are those in which a few fluxoids can nucleate before the sample makes a transition to the normal state. It was found that these disks: (1) exhibit a variety of phase transitions (type I or type II) that are absent in macroscopic samples; (2) show strong hysteresis behavior, and (3) in the field down sweep can exhibit paramagnetic behavior.

In our earlier work⁵ we presented a quantitative explanation of the magnetization of the different disks as function of increasing external magnetic field where we found that the disks are in the ground state. Axially symmetric solutions with a fixed angular momentum L were assumed and the nonlinear GL equations were solved for disks with a finite thickness. In increasing field the *Bean-Livingston* (BL) surface barrier, responsible for metastability, is destroyed by boundary roughness which explains why the system follows the ground state. The BL barrier arises from the fact that the superconducting currents around a vortex is in the opposite direction to the screening currents at the surface of the sample. This barrier does not allow the nucleation of vortices at the boundary, although the free energy is lowered when the vortex moves to the center of the sample.

The decreasing field behavior of the magnetization, which was not studied in our previous work, can be very different and can even show paramagnetic behavior. One of the reasons for this different behavior is that the BL barrier in this case is not destroyed by surface defects and consequently, the steady state is not necessarily the ground state but it can be an excited state determined by the history of the sample and the metastability created by the Bean-Livingston barrier. In this case we cannot assume L states and the problem is much more difficult.

The GL equations were outlined in Refs. 5,6 where it was also shown that the order parameter can be considered to be

uniform in the z direction which is a very good approximation for disks with thickness less than the coherence length. We use the Gauss-Seidel method to solve the nonlinear GL equation [Eq. (1) in Ref. 5] and the fast-Fourier transform to solve the three-dimensional (3D) Maxwell equation [Eq. (2) in Ref. 5]. We study the system in increasing and decreasing magnetic field by taking the order parameter of the previous magnetic field as input in our iterative procedure of solving the GL equations. This ensures that the system does not escape from the local minima leading to metastability.

As a typical case let us consider a FwFD [radius $R = 0.8 \mu\text{m}$, thickness $d = 0.134 \mu\text{m}$, coherence length $\xi(0) = 0.183 \mu\text{m}$ and penetration length $\lambda(0) = 0.07 \mu\text{m}$] with parameters comparable to one of the disks used in the experiment.⁴ The solution obtained by assuming axial symmetry is referred to as the 2D solution whereas the general solution without this assumption will be referred to as the 3D solution. Let us consider the 2D solution first. The dimensionless free energy G , in units of $H_c^2 V / 8\pi$ (Ref. 5) (here V is the volume of the sample), is shown in Fig. 1(b) by the thin solid curves as a function of the applied magnetic field for the different L states. The corresponding magnetization for these different L states is shown in Fig. 1(a) by the thin solid curves. Hence, from Fig. 1(b), it can be seen that up to a magnetic field of 42.6 G, the $L=0$ state is the ground state. Beyond this field the $L=1$ state becomes the ground state. As we increase the field higher L states become the lowest energy state and this continues as long as the free energy G is negative after which the system turns normal. The free energy of the ground state of the system is given by the thick solid curve in Fig. 1(b) and the corresponding magnetization by the thick solid curve in Fig. 1(a). However, the free energy and the magnetization in increasing magnetic field as given by the 3D solution is shown by the thick dotted curve in Fig. 1. Thus the 3D solution in increasing magnetic field, takes the system along a steady state that conserves L up to the point where the free energy is zero at which point a jump to a higher L state occurs. The free energy and magnetization curve in decreasing magnetic field as given by the 3D solution, is shown in Fig. 1 by the thick dashed curves.

The experimental results for the magnetization of the disk considered in Fig. 1 are shown in Fig. 2 for increasing (open circles) and decreasing (squares) field. These curves are plot-

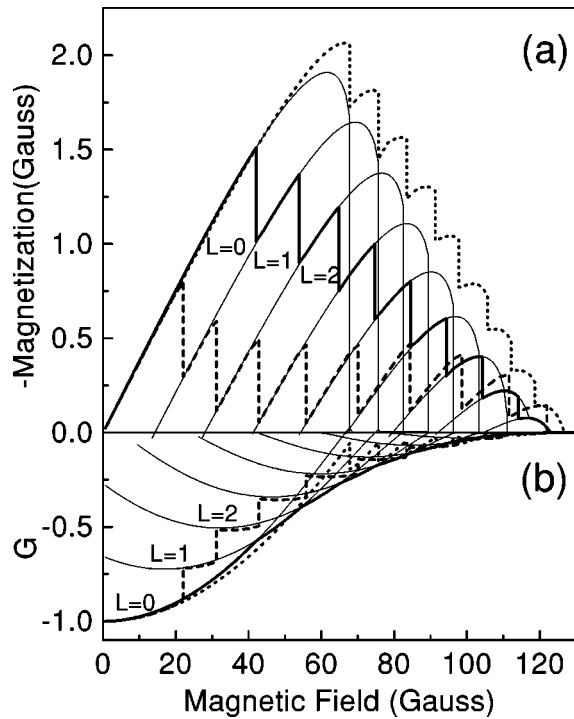


FIG. 1. The magnetization (a) and dimensionless free energy in units of $H_c^2 V / 8\pi$ (b) for a FwFD [radius $R=0.8 \mu\text{m}$, thickness $d=0.134 \mu\text{m}$, coherence length $\xi(0)=0.183 \mu\text{m}$ and penetration length $\lambda(0)=0.07 \mu\text{m}$] as a function of magnetic field. The thin solid curves are the 2D solutions for different L states. The ground state is given by the thick solid curve. The dotted and dashed curves are the increasing and decreasing field behavior obtained from the 3D solution.

ted according to the scale on the left y axis. The dashed and dotted curves in Fig. 2 are the thick solid and thick dashed curves of Fig. 1(a) but referred to the scale of the right y axis. Notice that the experimentally determined magnetization is a

factor of 25 smaller than the calculated sample magnetization. Furthermore in the experimental data, paramagnetic behavior is found for certain magnetic fields. Although diamagnetism is a fundamental property of superconductors, previously a paramagnetic Meissner effect⁷ was observed in large Nb disks. This discovery led to intensive research but the effect is still not completely understood.⁸ In the presence of pinning also superconducting samples can exhibit paramagnetic behavior. But we found that this discrepancy (i.e., the factor of 25 and the paramagnetic behavior) can be explained by considering the full experimental setup of Ref. 4.

The magnetometry used in the experimental work of Ref. 4 is explained in detail in Ref. 9. The superconducting sample is mounted on top of a small ballistic Hall cross and the magnetization of the superconducting disk was measured through the Hall effect. In Ref. 10 it was shown that the Hall voltage of a Hall cross, in the ballistic regime, is determined by the average magnetic field piercing through the Hall cross region. The Hall cross has a larger area than the sample and it measures the magnetization of this area rather than the magnetization of the sample. The field distribution in case of thin disks is extremely nonuniform inside as well as outside the disks and the detector size will have an effect on the measured magnitude of the magnetization, the nature and extent will depend on the magnetic-field profile. We calculated the magnetization measured by the detector by integrating the field expelled from the Hall cross. The detector was taken to be a square with width $3.1 \mu\text{m}$ which is placed just below the superconducting disk. The resulting magnetization is given by the solid curves in Fig. 2 drawn according to the scale on the left y axis i.e., with the same scale as the experimental data. Notice that by including the effect of the detector: (1) the magnetization is scaled down considerably, (2) the line shape is changed slightly, and (3) the detector output can give a positive magnetization although the sample itself is diamagnetic. These three factors bring the theoretical re-

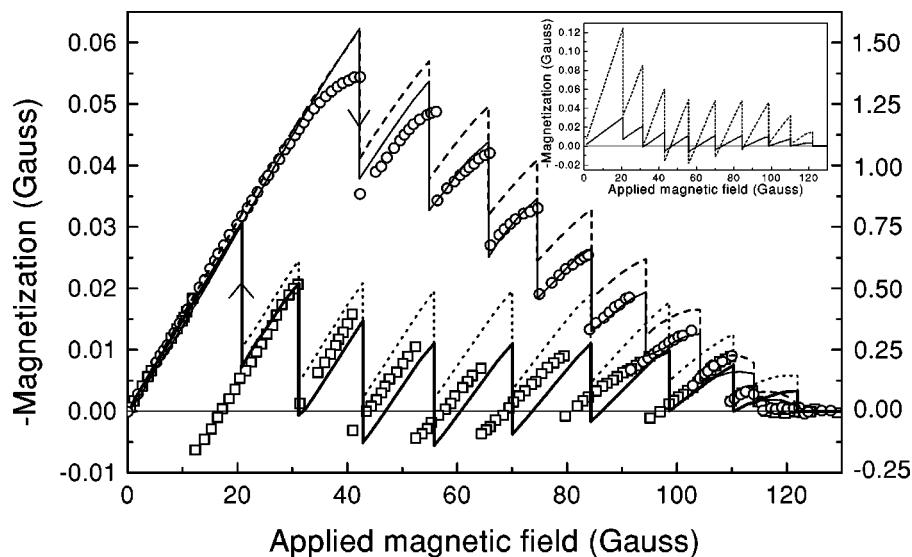


FIG. 2. The experimental results for the magnetization (left scale) in increasing (circles) and decreasing (squares) magnetic field for the disk of Fig. 1. Theoretical results for the sample magnetization (right scale) are given by the dashed and dotted curves. Inclusion of the detector size ($3.1 \mu\text{m} \times 3.1 \mu\text{m}$), gives the corresponding thin and thick solid curves with reference to the left scale. In the inset the dotted curve is the magnetization versus decreasing magnetic field for a detector size of $2 \mu\text{m} \times 2 \mu\text{m}$ whereas the solid curve is that for a detector size of $3.1 \mu\text{m} \times 3.1 \mu\text{m}$.

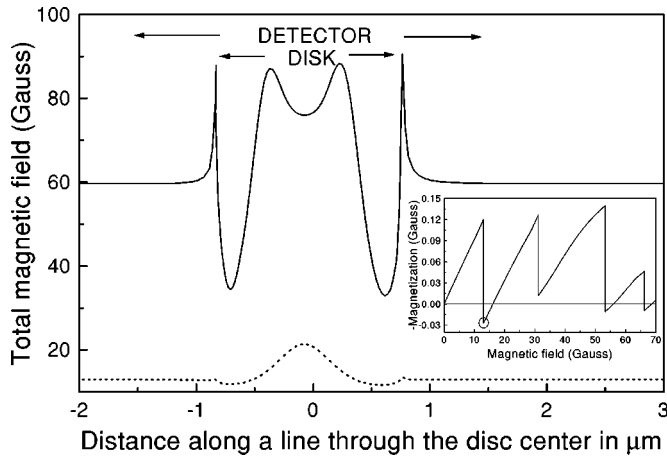


FIG. 3. The solid curve is the field distribution in case of an applied field of 59.65 G along a line through the center of the disk for the case of Fig. 1. The disk region and the detector region are indicated. The dotted curve is the corresponding result at an applied field of 13 G for a ten times thinner disk. The inset shows the magnetization versus decreasing applied field for this thin sample.

sult very close to the experimental result which explains even the apparent paramagnetic behavior. Only at the position of the last jump, in the field sweep down, there is a noticeable difference. This may be due to some pinning center near the center of the disk that becomes effective when the fluxoids inside shrink to the center. We found that decreasing the detector area enhances the apparent paramagnetic behavior. In the inset of Fig. 2 we compare the magnetization for a detector size of $2 \mu\text{m} \times 2 \mu\text{m}$ (dotted curve) with that for a detector size of $3.1 \mu\text{m} \times 3.1 \mu\text{m}$ (solid curve).

In order to understand why a larger detector can result in an apparent paramagnetic behavior we show in Fig. 3 the total magnetic field (applied field plus the field due to the magnetization of the sample) along a line passing through the center of the disk. Note that far away from the disk region the field is equal to the applied field of 59.65 G. This value was chosen because the detector magnetization shows a paramagnetic behavior in this case. In the center of the disk the magnetic field is much larger than the applied field because of the flux trapped by the BL barrier. Hence, the central region is paramagnetic. Near the edge of the disk, the magnetic field is much smaller than the applied field and is thus a diamagnetic region. In this region superconductivity is maximum and the disk is in the giant vortex state. The sample magnetization is the resultant magnetization of all these regions, and the total magnetization turns out to be diamagnetic. But when we calculate the magnetization determined by the detector, we have to include the magnetic field in the region outside the disk which is strongly paramagnetic. The magnetic field just outside the disk is larger than the applied field because of the strong flux expulsion from the disk and the important demagnetization effects in finite thickness disks. The $2 \mu\text{m}$ detector shows larger paramagnetism than the $3 \mu\text{m}$ detector due to the fact that over a very large area the net flux expelled should be zero. However, for sufficiently small detectors the paramagnetic behavior will disappear when its size becomes comparable to the sample size.

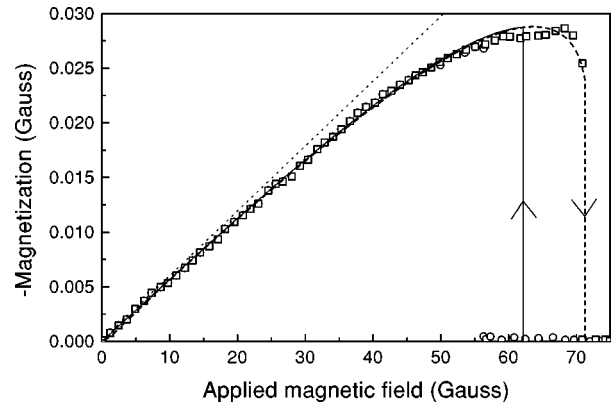


FIG. 4. The squares (circles) are the experimental data in increasing (decreasing) field for a FrFD [radius $R=0.5 \mu\text{m}$, thickness $d=0.15 \mu\text{m}$, coherence length $\xi(0)=0.25 \mu\text{m}$ and penetration length $\lambda(0)=0.07 \mu\text{m}$]. The dashed (solid) curve is the corresponding numerically calculated detector magnetization.

From the above discussion on the magnetic-field distribution in and around the superconducting disk we may ask whether it is possible to observe the superconductor in a state such that the paramagnetic region at the center has a larger contribution than the diamagnetic region near the boundary.⁸ In this case the sample itself would be paramagnetic. Indeed, we found that when the thickness of the sample is greatly reduced, the sample magnetization itself can be paramagnetic in a field down sweep. We reduced the thickness of the disc by a factor of 10 and kept all other parameters fixed which leads to the sample magnetization as shown in the inset of Fig. 3. The maximum paramagnetism is 0.027 G which occurs at 13 G as indicated by the circle in Fig. 3. For such a thin disk, the diamagnetic response is very small and the flux trapped inside the giant vortex state determines the sign of the response. The magnetic-field distribution for this case is given in Fig. 3 by the dotted curve. Notice the weak flux expulsion from the diamagnetic boundary and as a result the paramagnetic region outside the sample is negligible.

Next we consider a FrFD [radius $R=0.5 \mu\text{m}$, thickness $d=0.15 \mu\text{m}$, coherence length $\xi(0)=0.25 \mu\text{m}$ and penetration length $\lambda(0)=0.07 \mu\text{m}$] with a larger coherence length than the previous one, which is probably due to larger disorder in the disk. The disk shows (see Fig. 4) a first-order phase transition to the normal state. Its behavior in increasing field was explained in Ref. 5. Hysteresis in the case of this FrFD is different because the BL barrier cannot result in metastability here because this requires the presence of a vortex. In order to explain this hysteretic behavior we use the 2D solution because of its high accuracy and because it is correct in the absence of multiple vortices. The experimental data in increasing (squares) and decreasing (circles) field are shown in Fig. 4. The 2D solution in increasing and decreasing fields are given by the dashed and solid curves, respectively, where the detector size (width $2.9 \mu\text{m}$) is included in our calculations. The nonlinear line shape and the magnitude of the magnetization are nicely reproduced. A straight dotted line is drawn tangent to the experimental data at the origin as a guide to the eye in order to accentuate this nonlinear behavior.

The origin of this hysteresis is due to metastability created by a *volume barrier* and not the BL surface barrier. The free

energy has two local minima corresponding to two different values of the order parameter corresponding to the normal and superconducting states, respectively. These two minima are separated by a maximum which acts as a barrier when the system tries to switch from one minimum to the other at the critical point. To differentiate it from the surface barrier we call it volume barrier. In increasing field the position of the jump in magnetization coincides with that of the experiment but in decreasing field it does not. In decreasing field this position is extremely dependent on small fluctuations in the normal system where the order parameter is zero which is not the case in increasing field. In increasing field the order parameter (magnetization) in the superconducting state is large and the potential energy (linear and nonlinear term) dominates the free energy. Whereas in decreasing field the order parameter is zero before the jump, the potential energy is negligible and the gradient term, although small, is the only term contributing to the free energy. Hence, if the order parameter starts growing in some region of the sample, the neighboring regions try to destroy it because this will reduce the gradient term in the free energy. Therefore, starting from different initial conditions we obtain different positions where this jump occurs. If we start from smaller values of the

order parameter, the jump in magnetization moves towards smaller magnetic fields and consequently increases the hysteresis. The position of this jump can also be changed if we add random fluctuations. The position of the jump in Fig. 4 corresponds to the field when the volume barrier disappears.

In conclusion, we showed that the hysteresis observed in mesoscopic disks,⁴ can be explained by considering metastability resulting from energy barriers: in the FwFD it is the BL surface barrier, whereas in the FrFD it is the volume barrier. In the ground state the magnetization of those disks is diamagnetic. Sweeping down the magnetic field brings the system in metastable states which have a substantial smaller diamagnetic behavior and can even be paramagnetic for certain thin disks. The size of the detector has a substantial influence on the magnitude of the measured magnetization and can even change the sign of it.

This work was supported by the Flemish Science Foundation (FWO-VI) Grant No. G.0232.96, the European INTAS-93-1495-ext project, and the Belgian Inter-University Attraction Poles (IUAP-VI). P.S.D. was supported financially by the FWO-VI. Discussions with Dr. A. Geim are gratefully acknowledged.

*Electronic address: deo@uia.ua.ac.be

†Permanent address: Institute of Theoretical and Applied Mechanics, Russian Academy of Sciences, Novosibirsk 630090, Russia.

‡Electronic address: peeters@uia.ua.ac.be

¹G. D. Cody and R. E. Miller, Phys. Rev. Lett. **16**, 697 (1966), and references therein.

²A. S. Joseph and W. J. Tomasch, Phys. Rev. Lett. **12**, 219 (1964); R. W. DeBlois and W. DeSorbo, *ibid.* **12**, 499 (1964).

³C. P. Bean and J. D. Livingston, Phys. Rev. Lett. **12**, 14 (1964).

⁴A. K. Geim, I. V. Grigorieva, S. V. Dubonos, J. G. S. Lok, J. C. Maan, A. E. Filippov, and F. M. Peeters, Nature (London) **390**, 259 (1997).

⁵P. S. Deo, V. A. Schweigert, F. M. Peeters, and A. K. Geim, Phys. Rev. Lett. **79**, 4653 (1997).

⁶V. A. Schweigert and F. M. Peeters, Phys. Rev. B **57**, 13 817 (1998).

⁷D. J. Thompson, M. S. M. Minhaj, L. E. Wenger, and J. T. Chen, Phys. Rev. Lett. **75**, 529 (1995), and references therein.

⁸V. V. Moshchalkov, X. G. Qiu, and V. Bruyndoncx, Phys. Rev. B **55**, 11 793 (1997), and references therein.

⁹A. K. Geim, S. V. Dubonos, I. V. Grigorieva, J. G. S. Lok, and J. C. Maan, Appl. Phys. Lett. **71**, 2379 (1997).

¹⁰F. M. Peeters and X. Q. Li, Appl. Phys. Lett. **72**, 572 (1998).